

Organic & Biomolecular Chemistry

Accepted Manuscript



This is an *Accepted Manuscript*, which has been through the Royal Society of Chemistry peer review process and has been accepted for publication.

Accepted Manuscripts are published online shortly after acceptance, before technical editing, formatting and proof reading. Using this free service, authors can make their results available to the community, in citable form, before we publish the edited article. We will replace this *Accepted Manuscript* with the edited and formatted *Advance Article* as soon as it is available.

You can find more information about *Accepted Manuscripts* in the [Information for Authors](#).

Please note that technical editing may introduce minor changes to the text and/or graphics, which may alter content. The journal's standard [Terms & Conditions](#) and the [Ethical guidelines](#) still apply. In no event shall the Royal Society of Chemistry be held responsible for any errors or omissions in this *Accepted Manuscript* or any consequences arising from the use of any information it contains.

ARTICLE

Tricyclic dihydrobenzoxazepine and Tetracyclic indole derivatives can specifically target bacterial DNA ligases and can distinguish between the human DNA Ligase I

Cite this: DOI: 10.1039/x0xx00000x

Received 00th January 2012,

Accepted 00th January 2012

DOI: 10.1039/x0xx00000x

www.rsc.org/

Nisha Yadav^{1§}, Taran Khanam^{2§}, Ankita Shukla², Niyati Rai², Kanchan Hajela^{1#} and Ravishankar Ramachandran^{2*}

Abstract : DNA ligases are critical players of DNA metabolism in all organisms. NAD⁺-dependent DNA ligases (LigA) found exclusively in bacteria and certain entomopoxviruses are drawing increasing attention as therapeutic targets as they differ in their cofactor requirement from ATP-dependent eukaryotic homologs. Due to similarities in the co-factor binding sites of the two classes of DNA ligases, it is necessary to find determinants that can distinguish between them for exploitation of LigA as an anti-bacterial target. In the present endeavour, we have synthesized and evaluated a series of tricyclic dihydrobenzoxazepine and tetracyclic indole derivatives for their ability to distinguish between bacterial and human DNA ligases. The *in vivo* inhibition assays that employed LigA deficient *E. coli* GR501 and *S. typhimurium* LT2 bacterial strains, rescued by ATP-dependent T4 DNA ligase or *Mycobacterium tuberculosis* NAD⁺-dependent DNA ligase (Mtb LigA) respectively, showed that the compounds can specifically inhibit bacterial LigA. The *in vitro* enzyme inhibition assays using purified MtbLigA, human DNA ligase I & T4 DNA ligase showed specific inhibition of MtbLigA at low micromolar range. Our results demonstrate that the tricyclic dihydrobenzoxazepine and tetracyclic indole derivatives can distinguish between bacterial and human DNA ligases by ~5-folds. *In silico* docking and enzyme inhibition assays identified that the compounds bind to the co-factor binding site and compete with the cofactor. Ethidium bromide displacement and gel-shift assays showed that the inhibitors do not exhibit any unwanted general interactions with substrate DNA. The results set the stage for detailed exploration of this compound class for development as antibacterials.

Introduction

Emergence of resistance to bacterial infections is an emergent issue and we need to stay one step ahead of the game. The fight includes the discovery of anti-bacterials with new modes of action that can presumably avoid the present evasion tactics developed by bacterial pathogens. In infectious diseases like tuberculosis that affects a huge number of the world's population, it has become even more pressing. For *eg.* the combat against TB is protracted by the emergence of multidrug resistant (MDR) and extensively drug resistant (XDR) strains of *M. tuberculosis*¹ and comparative stagnation in the development of new antibiotics, particularly those that have novel modes of action.^{2, 3} Antibiotics in current use predominantly target a minuscule number of bacterial targets, largely affecting peptidoglycan, biosynthesis or gene expression/translation.⁴ However, the growing body of scientific evidences suggest that there remain many cellular targets, essential for the mycobacterial pathogen, which can be evaluated for therapeutic interference.

DNA metabolism is essential for bacterial survival, involving indispensable processes like DNA replication, DNA recombination, DNA repair and transcription. Under the 'common enzyme-diverse pathways' approach, there may be various opportunities for novel therapeutic interventions affecting one critical functional component that influences more than one vital life processes in the microbe.⁵ One such central target is DNA ligase that catalyzes joining of nicks between adjoining bases of duplex DNA at a single or double stranded break by mediating the formation of phosphodiester bonds between adjacent 5' phosphoryl and 3' hydroxyl groups. The first step is the formation of a covalent DNA ligase-adenylate intermediate where the AMP group is derived from the covalently bound cofactor, that can be ATP or NAD⁺.⁶ Subsequently, AMP is transferred from DNA ligase to the 5' phosphate of nicked DNA through a pyrophosphate bond. Finally, a phosphodiester bond is formed to join adjacent polynucleotides, with the release of AMP. DNA ligases are grouped under two classes based on the source of the AMP cofactor: NAD⁺-dependent DNA ligases present in bacteria, some entomopox viruses and mimi virus and ATP-dependent DNA ligases found in different viruses, archaea, eukaryotes and higher organisms.⁷⁻⁹

NAD⁺-dependent DNA ligase (LigA) has drawn attention in case of *Mycobacterium* as a target with the potential to combat multiple drug resistance because of its essential nature for bacterial viability, high conservation and discrete nature in terms of its architecture and cofactor requirement from the human homolog.^{7,10-12,13-17} The information gained by the structural studies of several DNA ligases in complex with their cofactors from prokaryotic and eukaryotic origins, show many similarities in the co-factor (ATP/NAD⁺) binding mode.^{15,17-21} The *Escherichia coli* DNA LigA structure in complex with AppDNA²² and structure of *Enterococcus faecalis* LigA¹⁵ with NAD⁺ has underscored the existence of a "druggable" active site harbouring hydrophobic tunnel extending from the nucleotidyl transferase domain to the adenosine-binding domain. In contrast, this tunnel is absent in ATP-dependent DNA ligase including human DNA ligase (HuLigI).²³ This subtle difference between the host and pathogen enzymatic machinery provides a platform for the development of specific and potent antibacterials targeting the druggable tunnel. This has prompted rational designing of small molecule inhibitors to find new prototypes that can act specifically against bacterial NAD⁺-dependent DNA ligases.²⁴⁻²⁸ Arylamine compounds and chloroquine derivatives are potent LigA inhibitors but they have the disadvantage of binding to DNA. Also, they do not compete with NAD⁺ binding and instead bind at some other target site.²⁹ Pyridochromanones on the other hand are competitive inhibitors of the enzyme.³⁰

Considering employment of human DNA ligase as an anti-cancer target in recent times,^{24,31-33} an anticipated challenge would be to distinguish between pathogen and host enzyme.

Our group has reported the identification of diverse compound families which inhibit bacterial NAD⁺-dependent DNA ligases with several fold specificity compared to ATP-dependent ligases including the human DNA ligase I.^{17,34,35} We have previously reported through virtual screening N-substituted tetracyclic indole as specific and potent inhibitor of NAD⁺ dependent DNA ligase.³⁴ As a part of our extended efforts we have synthesised a new series of tetracyclic compounds (indole and dihydrobenzoxazepine derivatives) with better predicted binding affinities based partially on the position of the water clusters.³⁴ We have evaluated the compounds for their potencies and cofactor specificities using a variety of *in vitro* assays involving purified enzymes, and *in vivo* assays involving LigA deficient bacterial strains. The docking and modelling studies attribute the inhibitor specificity to mimicking of NAD⁺-enzyme interaction. Overall, the *in vitro* and *in vivo* assays clearly demonstrate that these compounds can distinguish between NAD⁺ and ATP-dependent ligases and also that the *in vivo* mode of action is largely through inhibition of the essential LigA.

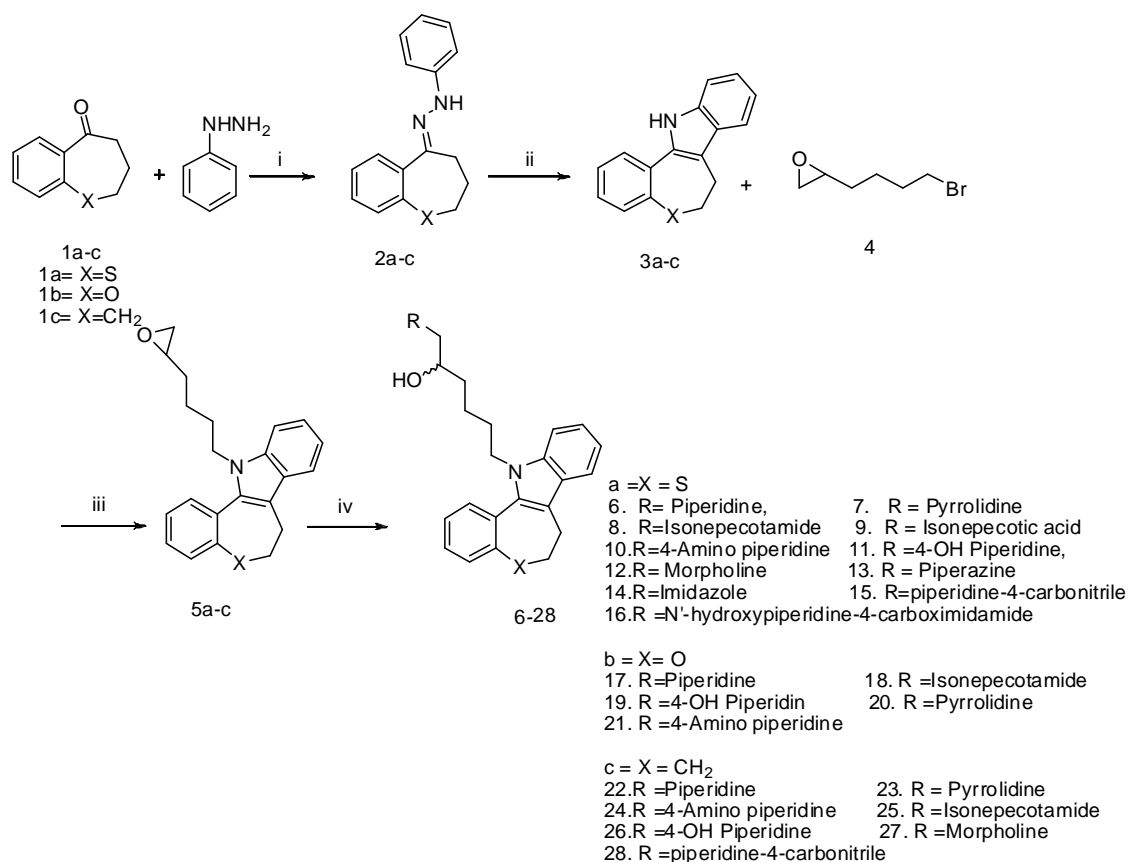
Results and Discussion

Chemistry

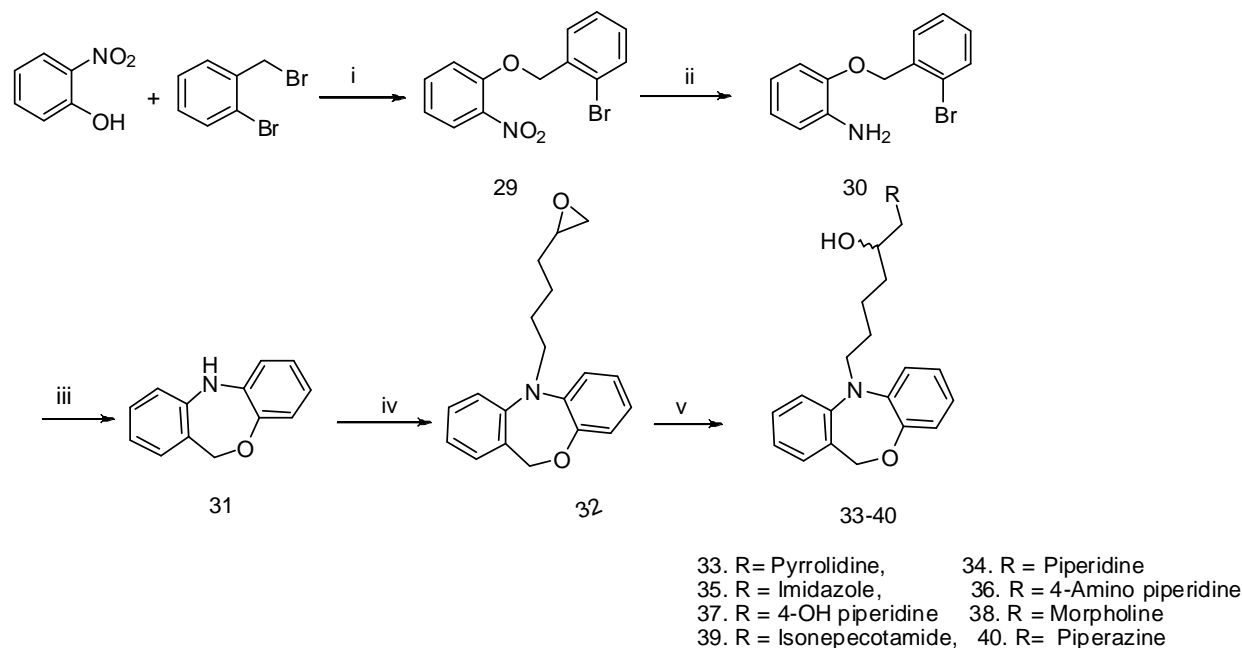
Three prototypes of compounds with different tricyclic and tetracyclic ring systems were synthesised and evaluated for their MtbLigA inhibitory activity. For the synthesis of prototype-I as shown in Scheme 1, the tetracyclic indoles namely, benzo[2,3]thiepine[4,5-b]indole, benzo[2,3]oxepino[4,5-b]indole and benzo[6,7]cyclohepta[1,2-b]indole **3a-c** which formed the core intermediates, were prepared by subjecting the phenyl hydrazones **2a-c** to Fisher indole synthesis³⁶. N-alkylation with commercially available 6-bromo-1,2-epoxyhexane **4** furnished the epoxides **5a-c** as solids in quantitative yields. Finally, opening of the epoxide ring with different secondary amines gave the desired target molecules **6-28** in good yields. All the final molecules were adequately characterised by spectral analysis.

The synthesis of N-alkylated dibenzoxazepine derivatives (prototype **II**) was commenced with the preparation of 5,11-dihydrodibenzo[b,e][1,4]oxazepine³⁷ **31**. Base catalysed alkylation of 2-nitrophenol with 2-bromo benzyl bromide in dry acetone under reflux conditions afforded the benzyl ether **29** in quantitative yield. Subsequent reduction of the 2-nitro group to 2-amino benzyl ether **30** followed by intramolecular Cu/L-Proline catalysed C-N coupling reaction yielded the dibenzoxepine **31** in 50% yield. The sequential N-alkylation with 6-bromo-1,2-epoxyhexane **4** followed by ring opening with different secondary amines (Scheme-2) provided the desired N-substituted dibenzoxepine derivatives **33-40** in excellent yields.

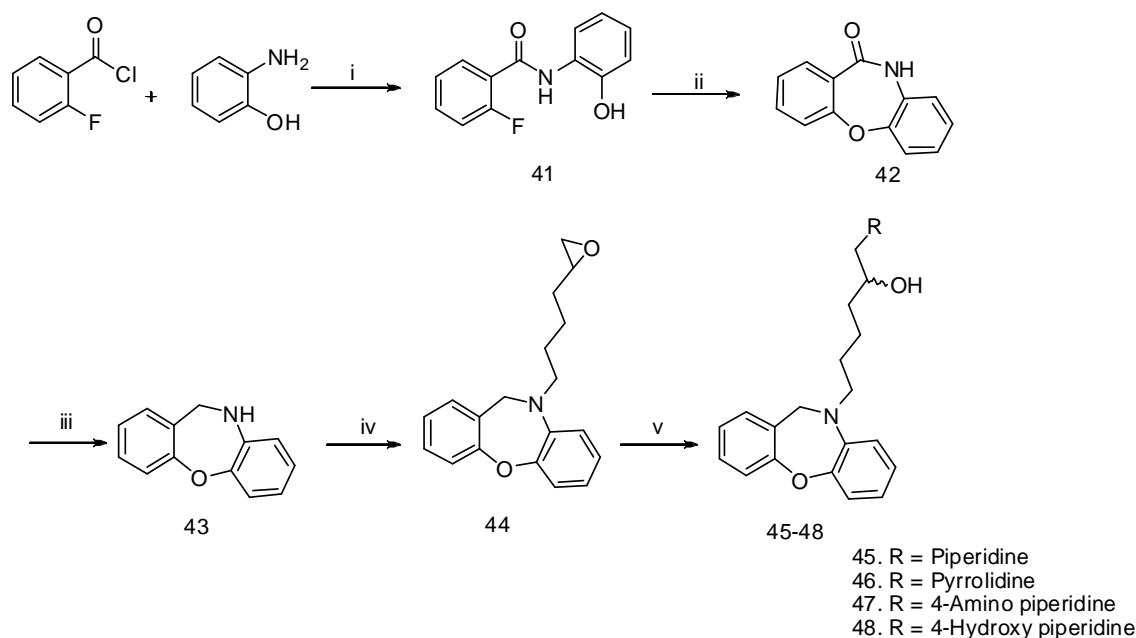
To synthesise the starting precursor, 10,11-dihydrodibenzo[b,f][1,4]oxazepine³⁸ **43** for the synthesis of prototype **III** compounds (scheme 3) was followed. N-acylation of 2-amino phenol with 2-fluoro-benzoyl chloride formed the 2-fluoro-N-(2-hydroxyphenyl)benzamide **41** which on etherification afforded the keto compound, dibenzo[b,f][1,4]oxazepin-11(10H)-one **42** in very good yields. Subsequent reduction of the amidic carbonyl with LAH provided the cyclised oxazepine **43** in excellent yield. Following the procedure of N-alkylation as described in Schemes 1 and 2, the target compounds **45-48** of prototype **III** were obtained in good to excellent yields (Scheme 3).



Scheme 1. Synthesis of prototype I molecules. Reagents and conditions: (i) Ethanol / glc.acetic acid, reflux 6h ; (ii) EtOH, 20% aq. HCl , 80-85 % ; (iii) NaH, dry DMF, 0°C, RT, 1h, 85- 90% ; (iv) 2° Amine, EtOH, reflux , 12 h, 70-78%.



Scheme 2. Synthesis of compounds of prototype II. Reagents and Conditions: (i) K₂CO₃, dry Acetone, reflux ,3h, 95% ; (ii) Fe/HCl, EtOH, reflux 4-5h, 78% ; (iii) CuI, L-Proline, t-BuOK, DMF, N₂, 110 °C, 24 h, 50% ; (iv)) NaH, 4, dry DMF, 0°C-RT, 1h, 85% ; (v) 2° Amine, EtOH, reflux , 12h, 68-75%.



Scheme 3. Synthesis of Compounds of Prototype III. Reagents and conditions ; (i) Et₃N, THF, 0°C-RT, 12h, 74%; (ii) NaOH, DMF, 120°C, 5h, 78%; (iii) LiAlH₄, THF, 70 °C, 85%; (iv) NaH, dry DMF, 0°C-RT, 1h, 88 %; (v) 2° Amine, EtOH, reflux , 12h, 70-75%.

In silico docking calculations. Control docking studies using AMP structure already present in crystal structure and Autodock 3.0.5 were performed as described earlier.³⁹ The reference molecule, AMP, adopted a similar conformation as reported in the crystal structure (**Fig. 1A**), validating the computational strategy. The conformations of the docked inhibitors were observed to be similar to the conformation of the AMP moiety occupying the same binding site (**Fig. 1B**). After the AutoDock simulations were complete, the binding energy of the docked inhibitor structures were analyzed (**Table 1**). Docking energy scores ranging from -12.9 to -10.6 kcal/mol were obtained, suggesting that the tested compounds might be inhibitors of the enzyme.

Hydrogen bonding parameters between the DNA ligase and the inhibitors were respectively visualized using PyMOL (v.1.2r3pre; Schrodinger LLC). The analysis highlighted some key residues that were consistently participating in the binding of all the inhibitors. Interactions for control AMP was also compared (**Fig 1A**). Leu90, Ser91, Leu92, Asn94, Glu121, Leu122, Lys123, Ala124, Ala128, Arg144, Arg182, Glu184, His236, Val298 and Lys300 were predicted to form hydrogen-bonding interactions with the compounds. Lys123, an essential residue, shows polar interactions with all the compounds that show good inhibition. Stacking interactions of the compounds with His236 appeared to be a characteristic feature of compound recognition in MtbLigA.

In vivo /antibacterial assays. Two bacterial systems were employed in order to evaluate the *in vivo* inhibition of NAD⁺ ligases, as previously reported.^{35,40} The first system used in the assays was a temperature sensitive *E.coli* GR501 strain that carries a *lig251* mutation in its LigA gene due to which it grows normally at 30°C. But its growth is strongly hampered at physiological temperatures. This deficiency is overcome by complementing it with NAD⁺ or ATP dependent ligases.⁴¹⁻⁴³ Consequently, this strain has been used

to study the *in vivo* specificity of inhibitors for LigA. We also used pTrc99A-based systems involving MtbLigA and T4Lig in this strain.⁴⁴

Next, to test whether the compounds also act upon NAD⁺ ligases from other bacterial sources, a well-known human pathogen, *S. typhimurium*, LT2 strain was used⁴⁵. Its DNA ligase null derivative TT1515 has been salvaged by T4 DNA ligase.⁴⁶ These two independent bacterial systems allowed us to explore the *in vivo* inhibition of LigA and ATP-dependent ligases by the given compounds.

The *E. coli* GR501 strain possessing only the pTrc99A plasmid demonstrated high sensitivity to the compounds (**Table 2**) compared to the corresponding ligase-complemented strains due to the remnant ligase activity in the mutant strain relative to the growth-rescued strains, which harbour a high copy number of the overexpressed ligase used to retrieve them. This is similar to observations in the case of pyridochromanones, glycosyl ureids, glycosyl amines, cycloalkanones etc.^{35,40,41} The results obtained after bactericidal studies done for the compounds demarcated eight compounds to be potentially active with low MIC values out of thirty five indole derivatives that were tested against MtbLigA. These eight compounds (**Table 2**) had ~1.5-3-fold lower MICs for the strain rescued by MtbLigA than for the strain rescued by T4 ligase. A similar trend was also observed in the case of *S. typhimurium* (**Table 2**). As revealed by the time kill studies, these compounds exhibited more sensitivity to the *S. typhimurium* wild-type LT2 strain harbouring the NAD⁺ dependent ligase compared to its ligase-deficient mutant TT1515, rescued by ATP-dependent ligase (**Fig. 2, S1**). The lower potency of inhibitors against ATP ligase rescued strains signifies that the inhibitory effect of compounds is unlikely to be an off-target effect. The *in-vivo* bactericidal studies aided us to screen potential compounds that

could discriminate between NAD^+ and ATP dependent DNA ligases for further *in-vitro* analysis.

In vitro enzymatic assays. To rapidly assess the potential of the synthesised compounds as specific inhibitors of MtbLigA, we performed assays where the eight indole/dihydrobenzoxepine compounds with low MICs, demarcated by bactericidal assays were examined at elevated concentrations (150 μM) against purified MtbLigA, T4 ligase and human DNA ligase I in respective ligation assays. Potential compounds that could discriminate between NAD^+ and ATP-dependent DNA ligases were thus identified for further analysis. Of the eight indole/dihydrobenzoxepine derivatives, compounds with $-\text{NH}_2$ groups at R_1 position and $-\text{OH}$ at R_2 position were able to distinguish better between two classes of enzymes by a factor of around 2. The results are summarized in **Table 1**. Although the cyclic indole/ dihydrobenzoxepine derived compounds inhibited MtbLigA with lesser IC_{50} values, the human DNA ligase I was much less sensitive to the compounds and was inhibited with IC_{50} values higher than 250 μM as shown in the **Table 1**.

In silico docking analysis suggested an overlap of the binding sites of NAD^+ and the synthesised indole and dihydrobenzoxepine derivatives. We, therefore, chose the best compounds **21**, **36** and **45** for standard kinetics analysis to explore their competitive action with respect to NAD^+ in *in-vitro* nick sealing assays. In the absence of the inhibitor, we determined a K_m of $1.7 \pm 0.2 \mu\text{M}$ for NAD^+ in the presence of 10% Me_2SO in the reaction mixture, which was in agreement with previously reported data^{35,40,47}. The analysis of the nick sealing assays in the presence of different concentrations of compounds **21**, **36** (0–250 μM) and **45** (0–100 μM) with increasing concentration of NAD^+ (0–60 μM) clearly indicated a competitive inhibition of NAD^+ by compounds, also revealed by their double reciprocal plots (**Fig. S2**, **S3** and **3**, respectively). The linear regression using the apparent K_m values lead to a K_i of 97.7 μM for compound **21** (**Fig. S1**), 94.2 μM and 56.6 μM for compound **36** and **45**, respectively (**Fig. S2** and **3**, respectively). These results clearly suggest that the binding sites of the cyclic indoles/ dihydrobenzoxepines overlaps with NAD^+ . Although all the three compounds **21**, **36**, and **45** showed competitive mode of inhibition compound **45** stands out as a potentially strong inhibitor of MtbLigA with significantly lower K_i value. The result is in agreement with the docking analysis which showed that compound **45** makes the largest number of hydrogen bonds/polar and hydrophobic interactions with the essential residues lining the cofactor binding site. The tricyclic indoles (**36** and **45**) also interact well with the NAD^+ binding site. The $-\text{OH}$ at R_2 position of **45** is involved in donor/acceptor interactions with the catalytic residue Glu184 while stacking interactions is seen between aromatic rings of the compound and His236 (**Fig. 1E**). The compound is also well positioned to exhibit interactions with critical residues like Lys300, Ser91, Arg 144 *etc.* However the introduction of $-\text{NH}_2$ group at position R_1 in compound **36** (**Fig. 1C**), results in loss of important interactions with the critical Lys 300 and Leu90 and might result in lower potency of the compound compared to **45**. The compound **21** (**Fig. 1D**) with bulky tetracyclic structure makes favourable interactions with few of the critical residues which make it active in our assays but it lacks important interactions with Lys300, Arg 144 and Leu 90 making it less potent than **45**.

DNA-Inhibitor Interaction Assays. We performed ethidium bromide displacement assays for the selected inhibitors in the current study to assess their interactions with DNA, if any. It was earlier reported that aryl amino compounds, a class of DNA ligase inhibitors, generally intercalate with DNA which might affect their inhibitory potencies⁴⁸. Maximum concentration of 250 μM (50 times

of EtBr) of respective compounds **21**, **36** and **45** were added in the reaction mixture containing EtBr-DNA and analysed by fluorescence spectra. We did not observe any marked displacement of ethidium bromide even at highest of compound's concentration (**Fig. S4, A, B, C**).

Gel shift assays were also performed to probe for any general inhibitor-DNA interactions, in the presence of increasing concentration of inhibitors. The results did not show any shift in the position of the DNA bands with increasing compound concentration, and clearly suggest that the cyclic indoles do not exhibit any general interactions with DNA (**Fig S4, D**).

Methods

In silico screening and docking. All the synthesized ligase inhibitors (**Fig. 1**) were constructed by full energy minimization using the BUILDER module in *Insight II* software (ver. 2000.1 Accelrys Inc.). The crystal structure of the adenylation domain of MtbLigA (PDB ID: 1ZAU) was used for docking after being shorn of the water molecules and heteroatoms. The binding pocket of DNA ligase is bordered by the residues Leu90, Ser91, Asn94, Glu121, Leu122, Lys123, Ala124, Arg144 and Glu184 respectively. The docking studies were carried out using Autodock 3.0.5.⁴⁹ The Kollman charges, solvation parameters and polar hydrogens were added and charges on residues were neutralized. The ligands were prepared for calculations by adding gasteiger charges. The cubic grid box size was set at $64 \text{ \AA} \times 54 \text{ \AA} \times 58 \text{ \AA}$ (x, y, and z) with spacing of 0.375 \AA , which included all the amino acid residues that were present in the catalytic site. AutoGrid 8 program was used to produce grid maps. The rest of the parameters were set to standard default values. The population size was set to 150 and the individuals were initialized randomly. A maximum of 20 poses were evaluated for each compound using the Lamarckian genetic algorithm (LGA), with the medium number of energy evaluations (250000). The Autodock results were analyzed to study the interactions and the binding energy of the respective docked structures.

Antibacterial Activity and Inhibition of Ligase *in vivo*. Two specific ligase deficient (*E. coli* and *S. typhimurium*) bacterial strains were employed to study the effect of inhibitors on their growth. The recombinant plasmid pRBL⁴⁴ carrying the gene for T4Lig in pTrc99A was transformed into temperature sensitive *E. coli* GR501 ligA^{ts} mutant⁴². The MtbLigA clone in pTrc99A was also transformed into *E. coli* GR501 so as to have the same genetic background.⁴⁰ The growth of strains expressing MtbLigA or T4Lig were compared with a control GR501 strain carrying empty pTrc99A without any gene insertions at 37°C. As reported earlier⁴¹ and reproduced by us, the temperature-sensitive *E. coli* GR501 ligA^{ts} strain grows well at 30°C, while robust impediment of growth occurs at 37°C. Complementation with either MtbLigA or T4Lig re-establishes the growth of the mutant strain.

As another system for investigating the specificity of inhibitors *in vivo* and to monitor their action against other NAD^+ -dependent DNA ligases, we used the *S. typhimurium* wild type LT2 strain and its DNA ligase deficient null derivative TT1515 which had been salvaged with a plasmid (pBR313/598/8/1b) encoding T4 ligase gene.⁴⁶ Minimum inhibitory concentrations (MICs) of the inhibitors were determined for both the above mentioned bacterial strains. The MIC values were determined in broth microdilution assays in microtiter plates in a volume of 200 μL . Serial 2-fold dilutions of antibacterial compounds were seeded with inoculums containing approximately 10^5 colony-forming units/ml in the case of the *E. coli* ligA^{ts} mutant and 10^6 colony-forming units/ml in the case

of *S. typhimurium* LT2 and its LigA⁻ mutant strain, rescued with T4 DNA ligase, under ambient conditions for 20 h. The MICs were inferred as the lowest concentrations of compounds that prevented visible microbial growth. The *E. coli* mutant strain was grown in LB medium, whereas the *S. typhimurium* strains were grown in nutrient broth. In the case of *E. coli* the medium contained 25 µg/ml polymyxin B nonapeptide (Sigma-Aldrich) to facilitate penetration of the inhibitors across the outer membrane.

Time-kill Studies. An exponentially growing culture of *S. typhimurium* LT2 and its DNA ligase-null mutant derivative in nutrient broth were treated at $A_{600} = 0.4$ with increasing inhibitor concentrations. The effect on growth and viability was investigated by monitoring the A_{600} and the number of CFU for 6-7 hours following the addition of the antibacterial compound. For quantification of the CFU, culture aliquots of both the strains were serially diluted in phosphate-buffered saline and plated on nutrient agar. After incubation for 16 h at 37 °C colonies were visible on the plate.

In vitro enzyme inhibition assays. DNA substrate used for performing the *in vitro* ligation activity assays was a 40 base pair duplex DNA containing a single stranded nick between bases 22 and 23 as reported earlier.^{17,34,35} Briefly, the substrate was generated using three oligonucleotides that annealed in Tris/EDTA buffer: viz. a 40 nucleotides long template oligomer (5'-ATG TCC AGT GAT CCA GCT AAG GTA CGA GTC TAT GTC CAG G-3'), to 18 nucleotides 5' 6-FAM labelled (5'-AGC TGG ATC ACT GGA CAT-3') and 22 nucleotides (5'-CCT GGA CAT AGA CTC GTA CCT T-3'). This fluorescently labelled, nicked 40 base-pair duplex DNA substrate was employed to investigate the *in vitro* inhibitory activity of diverse compounds against MtbLigA, bacteriophage T4Lig and human DNA ligase I. The quantities of the individual enzymes were optimized for comparable degree of ligation, lacking any inhibitor under the assay conditions.⁵⁰

Full-length MtbLigA was expressed and purified as earlier.⁴⁰ The assays were carried out using 2 ng of the purified protein. A standard ligation assay reaction mixture (20 µl) contained 50 mM Tris-HCl (pH 8.0), 10 mM MgCl₂, 5 mM DTT, 10% dimethyl sulfoxide (Me₂SO), 2 µM NAD⁺ and 2 pmol FAM labelled nicked duplex DNA substrate and different concentration of compounds. The reactions were assembled on ice, incubated at 25 °C for 60 minutes. The termination of reactions was done by adding 10 µl of the stop solution (98% formamide, 10 mM EDTA, 0.15% xylene cyanol and 0.15% bromophenol blue). Samples were heated for 5 minutes at 100 °C and chilled on ice before loading. The reaction products were resolved on 15% polyacrylamide gels containing 8 M urea 90 mM Tris borate and 2.5 mM EDTA. Gels were scanned using Image Quant LAS 4000 (M/s GE healthcare) and band intensities of the ligated product were measured and quantified using ImageQuantTL 8.1 software. Since all the compounds were soluble in 100% (CH₃)₂SO and encompassed one-tenth volume of the ligation reaction mixture, the control reaction too included 10% (CH₃)₂SO.

T4 DNA ligase assay was performed in reaction mixture containing 0.05 U of enzyme (Amersham), 2 pmol of labelled template and 66 µM ATP in 66 mM Tris-HCl, pH 7.6 mM MgCl₂, 10 mM DTT and 10% Me₂SO. The expression plasmid of Human DNA ligase I was transformed into *E. coli* BL21 (DE3) and protein was purified as illustrated previously.⁵⁰ The procedure used carrying out the ligation assay was same as described above. 2 µg protein was used in 50 mM Tris-HCl, pH 8.0, 10 mM MgCl₂, 5 mM DTT, 50 mg/ml BSA and 1 mM ATP.

Calculation of IC₅₀ values. Potency of the compounds was measured by determining its IC₅₀ values by adding appropriate concentrations of the compound to the reaction mixture prior to the addition of the substrate in *in vitro* ligation assays. The IC₅₀ values were determined by plotting the relative ligation activity versus inhibitor concentration and fitting to the equation: $V_i/V_0 = IC_{50} / (IC_{50} + [I])$ using GraphPad Prism software. V_0 and V_i correspond to rates of ligation in the absence and presence of inhibitor, respectively, and [I] represent the inhibitor concentration.

Mode of inhibition. The saturating substrate concentration for MtbLigA was determined by increasing the NAD⁺ concentration from 0 µM to 60 µM, employing *Michaelis-Menten* kinetics. K_m for NAD⁺ was determined in 10% (CH₃)₂SO using the above described assay procedure. The kinetics for different amount of compounds were determined using varying concentrations of NAD⁺ under standard assay conditions as described earlier.³⁵

The rate of the ligation reaction was determined based on the extents of ligation by scanning the gel using Image Quant LAS 4000. The data was plotted using *Michaelis-Menten* kinetics in Graph Pad Prism where the abscissa denoted NAD⁺ concentration and ordinate corresponded to the rate of ligation. Likewise, K_i values were determined by plotting the apparent K_m values against the respective compound concentrations. Mode of inhibition was determined through standard analysis of *Lineweaver-Burk* kinetics.

DNA-Inhibitor Interactions.

Ethidium Bromide Displacement Assay:- The intercalating properties of the antibacterial compounds were monitored by its ability to displace ethidium bromide from DNA by competing with it for DNA binding. The displacement of ethidium bromide from DNA was measured by monitoring the loss in the fluorescence occurring due to its detachment from the duplex DNA⁵¹. The reaction mixture contained 5 µg of calf thymus DNA, 5 µM ethidium bromide, 25 mM Tris-HCl (pH 8.0), 50 mM NaCl, and 1 mM EDTA in total volume of 100 µl. The fluorescence analysis of ethidium bromide was instantly done at excitation wavelength of 485 nm and emission wavelength of 612 nm using Perkin Elmer spectrofluorometer LS55.

Gel Shift Assay:- Gel shift assays were performed using 100 ng of plasmid DNA (pUC18, Stratagene) incubated with increasing concentrations of inhibitors in TE buffer for 1 hour at room temperature. Subsequently DNA shift was analysed on 1.5% agarose gel.

Conclusions

The present study was undertaken to probe for specific inhibitory action of the tetracyclic and tricyclic indole derivatives against MtbLigA. Overall the studies revealed that tetracyclic and tricyclic indole derivatives could distinguish between the two classes of ligases. The *in vivo* studies support that the possible mode of action of the compounds are due to inhibition of the essential LigA in the bacteria. The compounds also did not display general interactions with DNA and act by competing with the co-factor NAD⁺. The ongoing focus is on developing next generation derivatives that exhibit improved potency and specificity for LigA. Being smaller in size these molecules are suitable for further optimisation.

Experimental Section:

General procedure for the synthesis of target molecules:

The respective epoxy compounds and dry secondary amines (1.2 eq.) were dissolved in absolute ethanol (5-10 ml) and the solutions were refluxed under continuous stirring for 10-12 h. After

completion of the reaction, ethanol was removed under vacuum to give the crude products as coloured oily liquids. The crude compounds were purified by column chromatography using neutral alumina as adsorbent and MeOH/CHCl₃ as eluent to afford the pure products.

1. 6-(6,7-dihydro-12H-benzo[2,3]oxepino[4,5-b]indol-12-yl)-1-(piperidin-1-yl)hexan-2-ol (17): Colourless viscous liquid (150 mg, 72%). ¹H NMR (300 MHz, CDCl₃) δ 7.61-7.58 (d, J=7.6 Hz, 1H), 7.48-7.42 (m, 2H), 7.30-7.19 (m, 5H), 4.63-4.59 (t, J=6.4 Hz, 2H), 4.33-4.28 (t, J=7.3 Hz, 2H), 3.65-3.62 (m, 1H), 3.39 (brs, 2H), 3.08-3.04 (t, J=6.4 Hz, 2H), 2.67-2.66 (m, 2H), 2.27-2.25 (d, J=6.5 Hz, 2H), 2.08-2.03 (m, 3H), 1.83-1.80 (m, 5H), 1.78-1.65 (m, 4H). ¹³C NMR (50 MHz, CDCl₃) δ 142.3, 139.4, 137.3, 136.3, 133.0, 130.1, 127.9, 127.7, 127.3, 126.3, 121.6, 119.4, 118.3, 114.8, 114.3, 110.3, 67.7, 62.1, 54.4, 43.9, 34.6, 34.0, 33.0, 32.1, 29.6, 29.4, 29.2, 23.6, 22.9, 22.8. IR (Neat, cm⁻¹): 3401, 3019, 2941, 2399, 1606, 1384, 1215, 1083, 757, 669. ESI-MS: (m/z) = 419 [M+H]⁺. HRMS (ESI) exact mass calcd for [C₂₇H₃₄N₂O₂+H]⁺ 419.2620, found 419.2704.

2. 1-(4-aminopiperidin-1-yl)-6-(6,7-dihydro-12H-benzo[2,3]oxepino[4,5-b]indol-12-yl)hexan-2-ol (21): Light yellow viscous liquid (152 mg, 70% yield). ¹H NMR (300 MHz, CDCl₃) δ 7.60-7.58 (d, J=7.8 Hz, 1H), 7.47-7.41 (m, 2H), 7.31-7.14 (m, 5H), 4.62-4.58 (t, J=6.4 Hz, 2H), 4.31-4.26 (t, J=7.5 Hz, 2H), 3.08-3.03 (t, J=7.2 Hz, 2H), 2.93-2.89 (m, 4H), 2.73-2.69 (m, 3H), 2.39-2.27 (m, 4H), 2.18-1.98 (m, 3H), 1.43-1.39 (m, 4H). ¹³C NMR (50 MHz, CDCl₃) δ 157.2, 138.0, 128.3, 127.4, 126.9, 123.8, 123.1, 121.9, 119.5, 118.1, 114.0, 112.9, 110.3, 66.1, 63.9, 54.0, 51.0, 48.5, 44.5, 35.8, 34.3, 29.9, 29.7, 24.4, 22.8. IR (Neat, cm⁻¹): 3401, 3019, 2929, 1644, 1384, 1215, 1084, 758, 669. ESI-MS: (m/z) = 434 [M+H]⁺. HRMS (ESI) exact mass calcd for [C₂₇H₃₅N₃O₂+H]⁺ 435.2841, found 435.2645.

3. 1-(4-aminopiperidin-1-yl)-6-(dibenzo[b,e][1,4]oxazepin-5(11H)-yl)hexan-2-ol (36): Colourless viscous liquid (135 mg, 68%). ¹H NMR (300 MHz, CDCl₃) δ 7.31-7.28 (m, 2H), 7.11-6.69 (m, 3H), 6.84-6.79 (m, 3H), 5.31 (s, 2H), 3.77-3.73 (t, J=6.6 Hz, 2H), 3.59-3.56 (m, 1H), 2.93-2.68 (m, 3H), 2.22-2.18 (m, 5H), 1.81-1.66 (m, 4H), 1.40-1.27 (m, 5H). ¹³C NMR (50 MHz, CDCl₃) δ 150.9, 149.4, 136.1, 132.0, 129.3, 128.7, 123.0, 122.4, 121.1, 120.6, 119.8, 119.5, 69.8, 67.1, 65.8, 64.7, 53.7, 50.3, 34.4, 29.8, 27.7, 23.2. IR (Neat, cm⁻¹): 3400, 3019, 2928, 2399, 1602, 1489, 1384, 1215, 1084, 928, 757, 669. ESI-MS: (m/z) = 396 [M+H]⁺. HRMS (ESI) exact mass calcd for [C₂₄H₃₄N₃O₂+H]⁺ 396.2651, found 396.2573.

4. 1-(6-(dibenzo[b,e][1,4]oxazepin-5(11H)-yl)-2-hydroxyhexyl)piperidine-4-carboxamide (39): Light yellow viscous liquid (160 mg, 75%). ¹H NMR (300 MHz, CDCl₃) δ 7.31-7.28 (m, 2H), 7.11-6.99 (m, 3H), 6.80-6.78 (m, 3H), 5.79 (s, 1H), 5.57 (s, 1H), 5.31 (s, 2H), 3.77-3.73 (t, J=6.6 Hz, 2H), 3.61-3.60 (m, 1H), 3.02-2.99 (m, 1H), 2.79-2.15 (m, 4H), 1.91-1.83 (m, 4H), 1.79-1.74 (m, 4H), 1.70-1.66 (m, 4H). ¹³C NMR (50 MHz, CDCl₃) δ 177.7, 150.8, 149.3, 136.0, 131.9, 129.2, 128.6, 122.8, 122.3, 121.0, 120.5, 119.7, 119.3, 114.1, 69.7, 66.1, 64.2, 54.8, 51.5, 50.2, 42.5, 34.4, 33.8, 31.9, 31.6, 29.7, 29.5, 28.9, 27.6, 23.1, 22.7. IR (Neat, cm⁻¹): 3408, 3020, 2930, 2401, 1675, 1599, 1489, 1262, 1076, 928, 760, 670. ESI-MS: (m/z) = 424 [M+H]⁺. HRMS (ESI) exact mass calcd for [C₂₅H₃₄N₃O₃+H]⁺ 424.2600, found 424.2618.

5. 6-(dibenzo[b,e][1,4]oxazepin-5(11H)-yl)-1-(piperazin-1-yl)hexan-2-ol (40): Colourless viscous liquid (130 mg, 69%). ¹H NMR (300 MHz, CDCl₃) δ 7.12-7.02 (m, 2H), 6.80-6.59 (m, 3H), 6.54-6.50 (m, 3H), 5.32 (s, 2H), 3.76-3.72 (t, J=6.5 Hz, 2H), 3.62 (s, 1H), 3.13-2.61 (m, 4H), 2.59-2.50 (m, 2H), 2.30-2.18 (m, 5H), 1.69-1.38 (m, 5H). ¹³C NMR (50 MHz, CDCl₃) δ

150.8, 149.2, 135.9, 131.9, 129.2, 128.6, 122.8, 122.2, 120.9, 120.5, 119.6, 119.3, 69.6, 65.7, 64.7, 54.3, 50.23, 46.1, 34.4, 27.6, 23.1. IR (Neat, cm⁻¹): 3401, 3019, 2399, 1602, 1384, 1215, 1084, 928, 758, 669. ESI-MS: (m/z) = 382 [M+H]⁺. HRMS (ESI) exact mass calcd for [C₂₃H₃₂N₃O₂+H]⁺ 382.2495, found 382.2497.

6. 6-(dibenzo[b,f][1,4]oxazepin-10(11H)-yl)-1-(piperidin-1-yl)hexan-2-ol (45): Light yellow viscous liquid (130 mg, 68%). ¹H NMR (300 MHz, CDCl₃) δ 7.18-7.15 (m, 1H), 7.12-7.05 (m, 4H), 6.95-6.83 (m, 1H), 6.81-6.76 (m, 2H), 4.41 (s, 2H), 3.69 (s, 1H), 3.22-3.17 (t, J=7.2 Hz, 2H), 2.64-2.63 (m, 2H), 2.35-2.25 (m, 3H), 2.21-1.72 (m, 5H), 1.65-1.43 (m, 8H). ¹³C NMR (50 MHz, CDCl₃) δ 157.8, 148.1, 141.5, 130.4, 128.7, 128.3, 124.4, 123.6, 120.1, 65.6, 64.6, 54.8, 53.1, 34.8, 29.6, 27.9, 25.0, 23.6, 23.1. IR (Neat, cm⁻¹): 3401, 3019, 2928, 2399, 1601, 1384, 1215, 1084, 928, 758, 627. ESI-MS: (m/z) = 381 [M+H]⁺. HRMS (ESI) exact mass calcd for [C₂₄H₃₃N₂O₂+H]⁺ 381.2542, found 381.2543.

7. 6-(dibenzo[b,f][1,4]oxazepin-10(11H)-yl)-1-(pyrrolidin-1-yl)hexan-2-ol (46): Light yellow viscous liquid (130 mg, 71%). ¹H NMR (300 MHz, CDCl₃) δ 7.25-7.10 (m, 5H), 7.08-7.05 (m, 1H), 6.96-6.76 (m, 2H), 4.41 (s, 2H), 3.2 (s, 1H), 3.20-3.17 (m, 4H), 2.92-2.89 (m, 2H), 2.74-2.71 (m, 4H), 2.49-2.45 (m, 1H), 2.07-2.05 (m, 3H), 1.89-1.66 (m, 5H). ¹³C NMR (50 MHz, CDCl₃) δ 157.7, 148.1, 141.5, 139.2, 130.3, 128.7, 128.3, 124.4, 123.6, 121.8, 120.2, 120.1, 114.0, 67.5, 62.1, 54.8, 54.3, 53.2, 34.8, 33.8, 31.9, 29.5, 29.1, 28.9, 27.8, 23.4, 22.6. IR (Neat, cm⁻¹): 3400, 3018, 2927, 2399, 1602, 1384, 1215, 1084, 928, 758, 669. ESI-MS: (m/z) = 367 [M+H]⁺. HRMS (ESI) exact mass calcd for [C₂₃H₃₁N₂O₂+H]⁺ 367.2386, found 367.2378.

8. 1-(6-(dibenzo[b,f][1,4]oxazepin-10(11H)-yl)-2-hydroxyhexyl)piperidin-4-ol (48): Colourless viscous liquid (142 mg, 72%). ¹H NMR (300 MHz, CDCl₃) δ 7.40-7.34 (m, 1H), 7.24-7.14 (m, 4H), 7.04-6.99 (m, 1H), 6.87-6.80 (m, 2H), 4.47 (s, 2H), 3.82-3.75 (m, 2H), 3.60 (s, 1H), 3.28-3.20 (m, 2H), 3.00-2.98 (m, 1H), 2.77-2.75 (m, 2H), 2.50-2.41 (m, 3H), 2.39-1.96 (m, 6H), 1.71-1.66 (m, 4H). ¹³C NMR (50 MHz, CDCl₃) δ 158.1, 148.4, 141.8, 139.6, 130.8, 129.1, 128.7, 124.8, 124.0, 122.2, 120.5, 114.4, 66.7, 55.2, 54.2, 53.4, 51.1, 48.8, 35.27, 34.6, 34.18, 32.28, 30.05, 29.8, 29.7, 29.5, 29.3, 28.3, 23.5. IR (Neat, cm⁻¹): 3401, 3019, 2936, 2399, 1601, 1487, 1384, 1215, 1059, 928, 757, 669. ESI-MS: (m/z) = 397 [M+H]⁺. HRMS (ESI) exact mass calcd for [C₂₄H₃₃N₂O₃+H]⁺ 397.2491, found 397.2487.

Acknowledgements

¹TK and NY are recipients of CSIR senior research fellowships.

²The work was funded by the Council of Scientific and Industrial Research, India, through SPLenDID [BSC0113] and GENESIS [BSC0104] grants respectively.

³This manuscript bears the CSIR-CDRI communication number 09/2014/RR.

⁴The abbreviations used are: *M. tuberculosis* LigA, MtbLigA; Adenosine triphosphate, ATP; Nicotinamide adenine dinucleotide, NAD⁺; Minimum inhibitory concentration, MIC; Ethidium bromide, EtBr

Notes and references

[§]These authors contributed equally to the paper.

¹From Medicinal and Process Chemistry, ²From the Molecular and Structural Biology Division, CSIR-Central Drug Research Institute, Sector 10, Jankipuram Extension, Sitapur Road, Uttar Pradesh, Lucknow-226031, India.

*To whom correspondence regarding biology should be addressed.

Ravishankar Ramachandran, Molecular and Structural Biology Division, CSIR-Central Drug Research Institute, Sector 10, Jankipuram Extension, Lucknow, Uttar Pradesh 226031, India, Tel:+91-522-2771940; Fax:+91-522-2771941; Email: r_ravishankar@cdri.res.in

#To whom correspondence regarding chemistry should be addressed

Kanchan Hajela, Medicinal and Process Chemistry Division, CSIR-Central Drug Research Institute Sector 10, Janakipuram Extension, Lucknow, Uttar Pradesh 226031, India, Tel:+91-522-2771940; Fax:+91-522-2771941; Email: kanchan_hajela@cdri.res.in

- M. Jassal and W. R. Bishai, *Lancet Infect. Dis.*, 2009, 9, 19-30.
- K. Duncan and C. E. Barry, 3rd, *Curr. Opin. Microbiol.*, 2004, 7, 460-465.
- Y. L. Janin, *Bioorg. Med. Chem.*, 2007, 15, 2479-2513.
- R. P. Lange, H. H. Locher, P. C. Wyss and R. L. Then, *Curr. Pharm. Des.*, 2007, 13, 3140-3154.
- T. Khanam and R. Ramachandran, *J. Indian I. Sci.*, 2014, 94, 149-168.
- M. A. Petit and S. D. Ehrlich, *Nucleic Acids Res*, 2000, 28, 4642-4648.
- A. Wilkinson, J. Day and R. Bowater, *Mol. microbiol.*, 2001, 40, 1241-1248.
- V. Sriskanda and S. Shuman, *J. Biol. Chem.*, 2002, 277, 9661-9667.
- J. Lu, J. Tong, H. Feng, J. Huang, C. L. Afonso, D. L. Rock, F. Barany and W. Cao, *Biochim Biophys Acta.*, 2004, 1701, 37-48.
- M. Korycka-Machala, E. Rychta, A. Brzostek, H. R. Sayer, A. Rumijowska-Galewicz, R. P. Bowater and J. Dziadek, *Antimicrob. Agents Chemother.*, 2007, 51, 2888-2897.
- S. Shuman, *Structure*, 2004, 12, 1335-1336.
- A. E. Tomkinson, S. Vijayakumar, J. M. Pascal and T. Ellenberger, *Chem. Rev.*, 2006, 106, 687-699.
- P. J. O'Brien and T. Ellenberger, *J. Biol. Chem.*, 2004, 279, 9750-9757.
- M. R. Singleton, K. Hakansson, D. J. Timson and D. B. Wigley, *Structure*, 1999, 7, 35-42.
- K. S. Gajiwala and C. Pinko, *Structure*, 2004, 12, 1449-1459.
- J. Y. Lee, C. Chang, H. K. Song, J. Moon, J. K. Yang, H. K. Kim, S. T. Kwon and S. W. Suh, *EMBO J.*, 2000, 19, 1119-1129.
- S. K. Srivastava, R. P. Tripathi and R. Ramachandran, *J Biol. Chem.*, 2005, 280, 30273-30281.
- S. Han, J. S. Chang and M. Griffor, *Acta Crystallogr. Sect. F Struct. Biol. Cryst. Commun.*, 2009, 65, 1078-1082.
- M. Odell, V. Sriskanda, S. Shuman and D. B. Nikolov, *Mol. Cell*, 2000, 6, 1183-1193.
- T. Ellenberger and A. E. Tomkinson, *Annu. Rev. Biochem.*, 2008, 77, 313-338.
- A. J. Doherty and S. W. Suh, *Nucleic Acids Res.*, 2000, 28, 4051-4058.
- J. Nandakumar, P. A. Nair and S. Shuman, *Mol. cell*, 2007, 26, 257-271.
- J. M. Pascal, P. J. O'Brien, A. E. Tomkinson and T. Ellenberger, *Nature*, 2004, 432, 473-478.
- N. Dwivedi, D. Dube, J. Pandey, B. Singh, V. Kukshal, R. Ramachandran and R. P. Tripathi, *Med. Res. Rev.*, 2008, 28, 545-568.
- S. D. Mills, A. E. Eakin, E. T. Burman, J. V. Newman, N. Gao, H. Huynh, K. D. Johnson, S. Lahiri, A. B. Shapiro, G. K. Walkup, W. Yang and S. S. Stokes, *Antimicrob. Agents Chemother.*, 2011, 55, 1088-1096.
- S. S. Stokes, M. Gowravaram, H. Huynh, M. Lu, G. B. Mullen, B. Chen, R. Albert, T. J. O'Shea, M. T. Rooney, H. Hu, J. V. Newman and S. D. Mills, *Bioorg. Med. Chem. Lett.*, 2012, 22, 85-89.
- S. S. Stokes, H. Huynh, M. Gowravaram, R. Albert, M. Cavero-Tomas, B. Chen, J. Harang, J. T. Loch, 3rd, M. Lu, G. B. Mullen, S. Zhao, C. F. Liu and S. D. Mills, *Bioorg. Med. Chem. Lett.*, 2011, 21, 4556-4560.
- W. Gu, T. Wang, F. Maltais, B. Ledford, J. Kennedy, Y. Wei, C. H. Gross, J. Parsons, L. Duncan, S. J. Arends, C. Moody, E. Perola, J. Green and P. S. Charifson, *Bioorg. Med. Chem. Lett.*, 2012, 22, 3693-3698.
- G. Ciarocchi, D. G. MacPhee, L. W. Deady and L. Tilley, *Antimicrob. Agents Chemother.*, 1999, 43, 2766-2772.
- H. Brotz-Oesterhelt, I. Knezevic, S. Bartel, T. Lampe, U. Warnecke-Eberz, K. Ziegelbauer, D. Habich and H. Labischinski, *J. Biol. Chem.*, 2003, 278, 39435-39442.
- L. Haracska, R. E. Johnson, I. Unk, B. Phillips, J. Hurwitz, L. Prakash and S. Prakash, *Mol. Cell. Biol.*, 2001, 21, 7199-7206.
- D. K. Singh, S. Krishna, S. Chandra, M. Shameem, A. L. Deshmukh and D. Banerjee, *Med. Res. Rev.*, 2014, 34, 567-595.
- W. J. Gui, S. Q. Lin, Y. Y. Chen, X. E. Zhang, L. J. Bi and T. Jiang, *Biochem. Biophys. Res. Commun.*, 2011, 405, 272-277.
- S. K. Srivastava, D. Dube, V. Kukshal, A. K. Jha, K. Hajela and R. Ramachandran, *Proteins*, 2007, 69, 97-111.
- S. K. Srivastava, D. Dube, N. Tewari, N. Dwivedi, R. P. Tripathi and R. Ramachandran, *Nucleic Acids Res.*, 2005, 33, 7090-7101.
- P. J. Luncsford, B. A. Manvilla, D. N. Patterson, S. S. Malik, J. Jin, B. J. Hwang, R. Gunther, S. Kalvakolanu, L. J. Lipinski, W. Yuan, W. Lu, A. C. Drohat, A. L. Lu and E. A. Toth, *DNA repair*, 2013, 12, 1043-1052.
- Dianova, II, V. A. Bohr and G. L. Dianov, *Biochemistry*, 2001, 40, 12639-12644.
- R. A. Bennett, D. M. Wilson, 3rd, D. Wong and B. Demple, *Proc. Natl. Acad. Sci. U. S.A.*, 1997, 94, 7166-7169.
- V. Kukshal, M. Mishra, A. Ajay, T. Khanam, R. Sharma, D. Dube, D. Chopra, R. P. Tripathi and R. Ramachandran, *Med. Chem. Comm.*, 2012, 3, 453-461.
- S. K. Srivastava, R. P. Tripathi and R. Ramachandran, *J. Biol. Chem.*, 2005, 280, 30273-30281.

41. H. Brotz-Oesterhelt, I. Knezevic, S. Bartel, T. Lampe, U. Warnecke-Eberz, K. Ziegelbauer, D. Habich and H. Labischinski, *J. Biol. Chem.*, 2003, 278, 39435-39442.
42. M. Lavesa-Curto, H. Sayer, D. Bullard, A. MacDonald, A. Wilkinson, A. Smith, L. Bowater, A. Hemmings and R. P. Bowater, *Microbiol.*, 2004, 150, 4171-4180.
43. A. Wilkinson, H. Sayer, D. Bullard, A. Smith, J. Day, T. Kieser and R. Bowater, *Proteins*, 2003, 51, 321-326.
44. Z. J. Ren, R. G. Baumann and L. W. Black, *Gene*, 1997, 195, 303-311.
45. U. E. Park, B. M. Olivera, K. T. Hughes, J. R. Roth and D. R. Hillyard, *J. Bacteriol.*, 1989, 171, 2173-2180.
46. G. G. Wilson and N. E. Murray, *J. Mol. Biol.*, 1979, 132, 471-491.
47. C. Gong, A. Martins, P. Bongiorno, M. Glickman and S. Shuman, *J. Biol. Chem.*, 2004, 279, 20594-20606.
48. G. Ciarrocchi, D. G. MacPhee, L. W. Deady and L. Tilley, *Antimicrob. Agents Chemother.*, 1999, 43, 2766-2772.
49. T. A. Ranalli, S. Tom and R. A. Bambara, *J. Biol. Chem.*, 2002, 277, 41715-41724.
50. S. Tom, L. A. Henricksen and R. A. Bambara, *J. Biol. Chem.*, 2000, 275, 10498-10505.
51. D. J. Hosfield, C. D. Mol, B. Shen and J. A. Tainer, *Cell*, 1998, 95, 135-146.

Table 1: *In vitro* inhibition of MtbLigA (NAD⁺dependent), T4 DNA ligase, and human DNA ligase I (ATP-dependent) by the respective compounds and their docking energies.

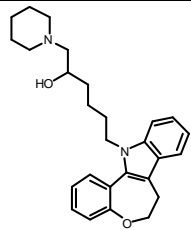
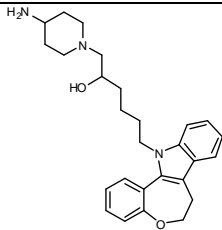
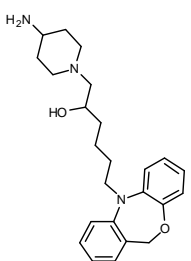
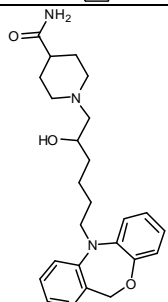
IC ₅₀ (μ M)					
S.No	Compound No	¹ MtbLigA	T4Lig	HuLigI	Docking energies ² (kcal/mol)
1	17	>100	>240	285 \pm 6	-12.5
2	21	65 \pm 5	110 \pm 8	274 \pm 9	-12.9
3	36	70 \pm 3	110 \pm 6	245 \pm 6	-12.3
4	39	>200	>300	ND ³	-12.6
5	40	200	>300	ND	-11.0
6	45	35.2 \pm 3	150 \pm 10	282 \pm 6	-12.1
7	46	>100	>250	278 \pm 5	-10.6
8	48	>200	>300	ND	-12.4

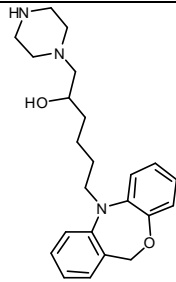
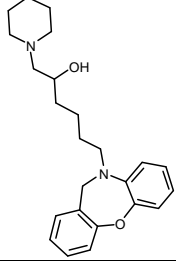
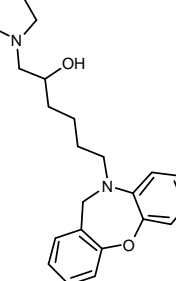
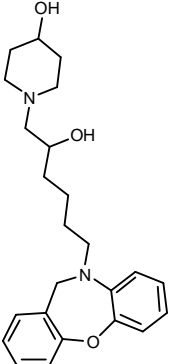
¹Mtb, *M. tuberculosis*

²Docking energies were calculated for respective compounds and Mtb NAD⁺-dependent DNA ligase by Autodock 3.0.5 as described in Methods

³ND, not determined.

Table 2: Antibacterial activity of the Tricyclic dihydrobenzoxazepine and Tetracyclic indole derivative

Compound No.	Compound's structure	MIC				
		<i>E.coli</i> GR501+ pTrc99A	<i>E.coli</i> GR 501+ <i>Mtb</i> NAD ⁺ ligase	<i>E.coli</i> GR501+ T4 DNA ligase	<i>S.typhimurium</i> LT2	<i>S.typhimurium</i> TT15151
17		0.4	15	25	30	>100
21		0.4	10	40	20	50
36		0.4	12	24	15	20
39		0.6	16	60	12	25

40		0.4	10	30	10	12
45		0.6	16	24	16	32
46		0.5	12	20	12	32
48		0.5	10	60	15	21

*The MIC values are given in $\mu\text{g/ml}$. The strains used in the study are explained in the text.

All compounds except for the ones listed in the table were tested from 0-200 $\mu\text{g/ml}$ concentration but they did not show any inhibitory activity.

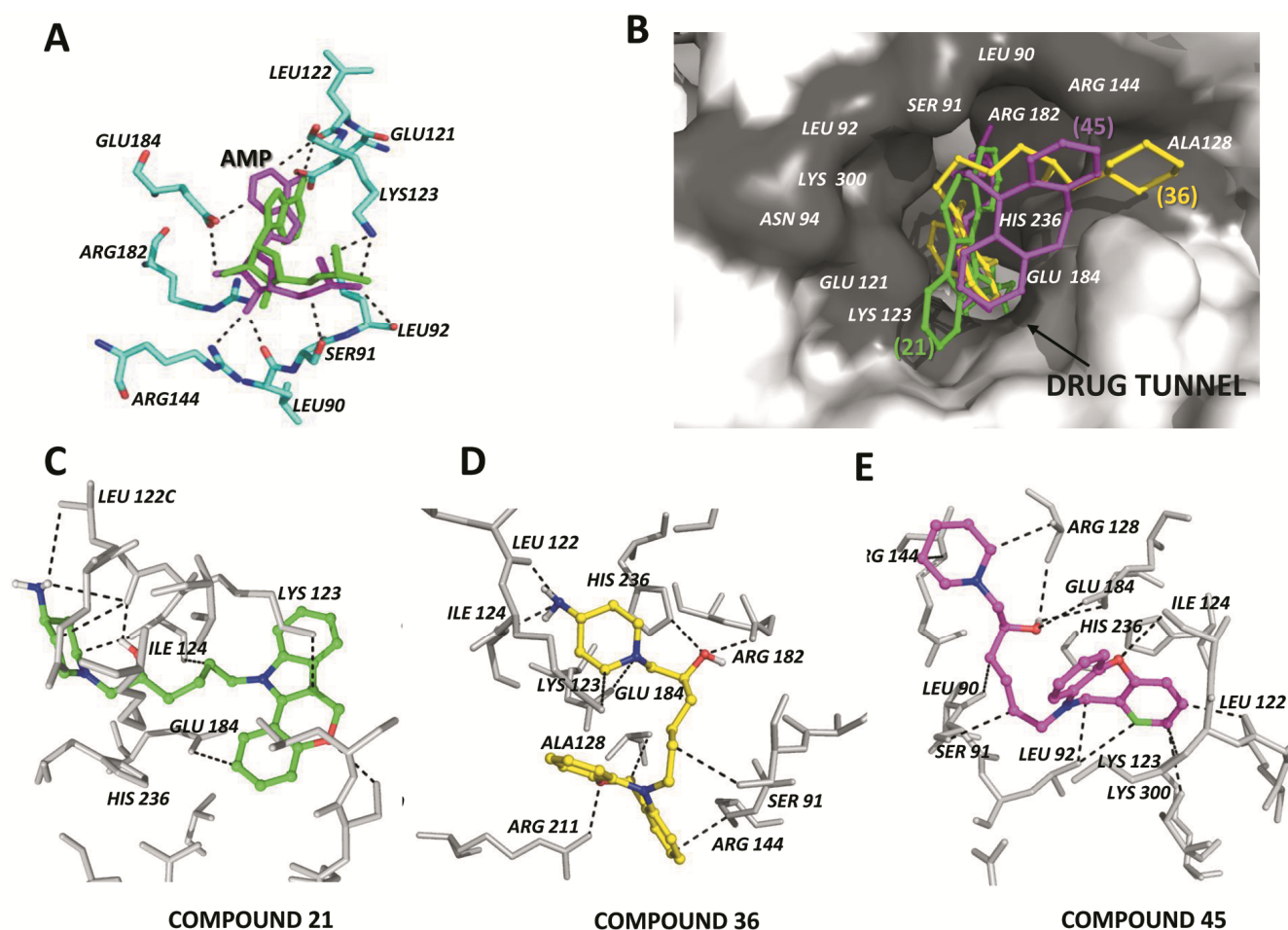


Figure. 1 Docking analysis: (A) Docking of AMP in the catalytic site. AMP in the crystal structure (Green sticks) and docked AMP (Magenta sticks) exhibit similar conformation. Active site residues are depicted as ball-and-sticks and are labeled in black. Hydrogen bonds are shown as dashed lines (B) Surface representation of DNA Ligase showing inhibitor **21** (pale Green), **36** (yellow) and **45** (magenta) sticks docked into the binding cleft of the protein. Protein has surface representation shown in white and dark grey denotes the substrate binding cleft. (C) Docked confirmations of inhibitor **21**(pale green stick) at the binding cleft. (D) Docked confirmations of inhibitor **36** (yellow stick) at the binding cleft. (E) Docked confirmations of inhibitor **45** (magenta stick) at the binding cleft. Active site residues are depicted as ball-and-sticks and are labeled in black. Bond interactions are shown in dashed lines.

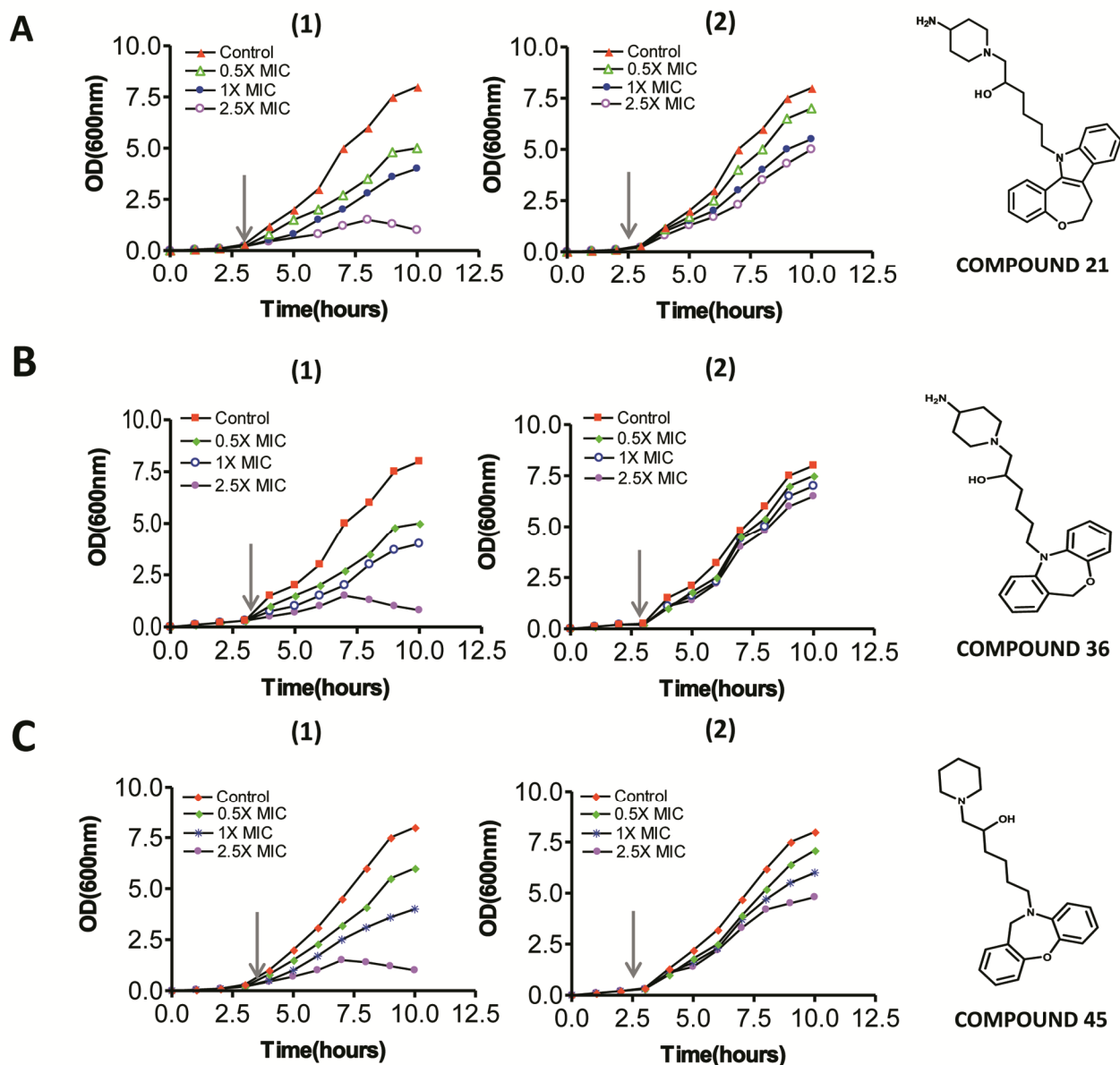


Figure 2: Bactericidal activity of Compounds (A) 21 (B) 36 (C) 45. Effect on growth as reflected in changes of the optical density at 600nm of (1) *S. typhimurium* LT2 and (2) its DNA ligase minus (null) derivative TT15151 [$\text{Lig}^- / \text{T4 Lig}^+$] on their respective exposures to compounds in $\mu\text{g/ml}$ representing 0.5 to 2.5 times the MIC value. The arrow indicates the point at which the compound was added. The structures of the respective compounds are shown beside the graphical representation of the experiments.

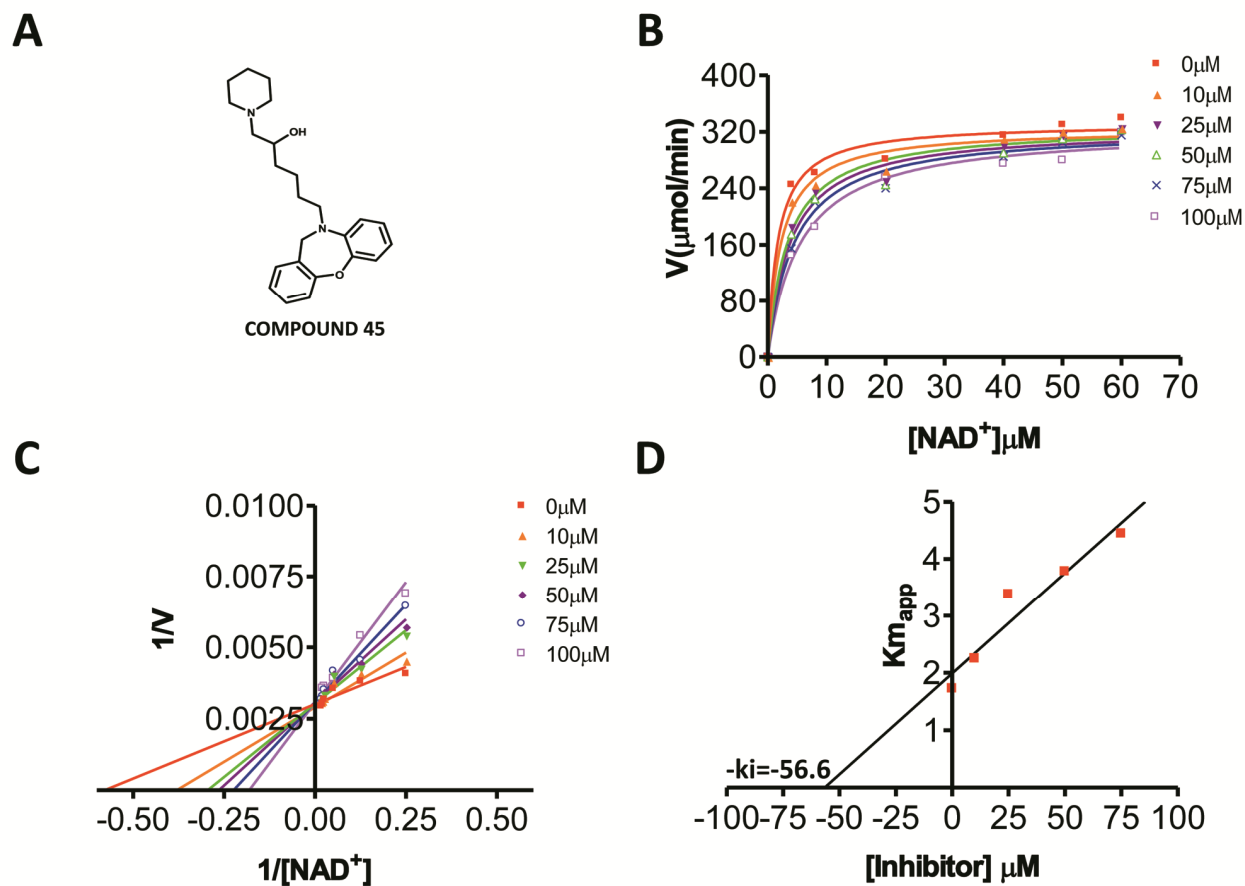


Figure 3: Competitive inhibition of MtbLigA with respect to NAD^+ by the Compound 45. (A) Structure of compound 45. (B) Activity of MtbLigA measured in the presence of rising concentrations of Compound 45 (0-100 μM) and NAD^+ (0 – 50 μM). (C) The double reciprocal plot shows competitive binding between NAD^+ and Compound 45. (D) K_i value for the Compound 45 was calculated to be 56.6 μM .

Table 1: *In vitro* inhibition of MtbLigA (NAD⁺dependent), T4 DNA ligase, and human DNA ligase I (ATP-dependent) by the respective compounds and their docking energies.

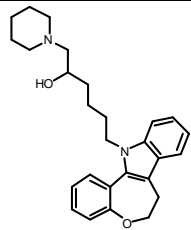
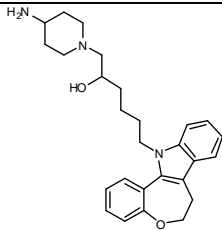
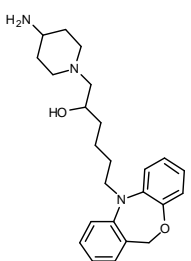
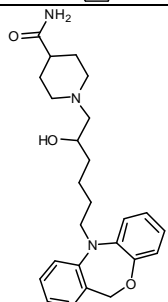
IC ₅₀ (μ M)					
S.No	Compound No	¹ MtbLigA	T4Lig	HuLigI	Docking energies ² (kcal/mol)
1	17	>100	>240	285 \pm 6	-12.5
2	21	65 \pm 5	110 \pm 8	274 \pm 9	-12.9
3	36	70 \pm 3	110 \pm 6	245 \pm 6	-12.3
4	39	>200	>300	ND ³	-12.6
5	40	200	>300	ND	-11.0
6	45	35.2 \pm 3	150 \pm 10	282 \pm 6	-12.1
7	46	>100	>250	278 \pm 5	-10.6
8	48	>200	>300	ND	-12.4

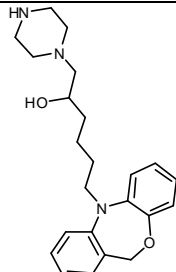
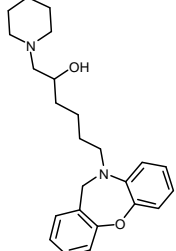
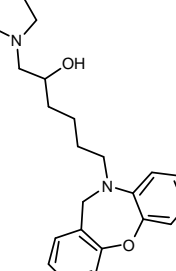
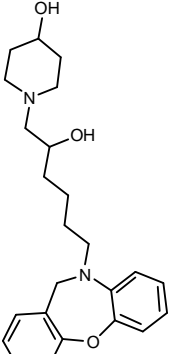
¹Mtb, *M. tuberculosis*

²Docking energies were calculated for respective compounds and Mtb NAD⁺-dependent DNA ligase by Autodock 3.0.5 as described in Methods

³ND, not determined.

Table 2: Antibacterial activity of the Tricyclic dihydrobenzoxazepine and Tetracyclic indole derivative

Compound No.	Compound's structure	MIC				
		<i>E.coli</i> GR501+ pTrc99A	<i>E.coli</i> GR501+ <i>Mtb</i> NAD ⁺ ligase	<i>E.coli</i> GR501+ T4 DNA ligase	<i>S.typhimurium</i> LT2	<i>S.typhimurium</i> TT15151
17		0.4	15	25	30	>100
21		0.4	10	40	20	50
36		0.4	12	24	15	20
39		0.6	16	60	12	25

40		0.4	10	30	10	12
45		0.6	16	24	16	32
46		0.5	12	20	12	32
48		0.5	10	60	15	21

*The MIC values are given in $\mu\text{g/ml}$. The strains used in the study are explained in the text.

All compounds except for the ones listed in the table were tested from 0-200 $\mu\text{g/ml}$ concentration but they did not show any inhibitory activity.